

Measurement of the $B^\pm \rightarrow \rho^\pm \pi^0$ Branching Fraction and Direct CP Asymmetry

B. Aubert,¹ M. Bona,¹ D. Boutigny,¹ F. Couderc,¹ Y. Karyotakis,¹ J. P. Lees,¹ V. Poireau,¹ V. Tisserand,¹
A. Zghiche,¹ E. Grauges,² A. Palano,³ J. C. Chen,⁴ N. D. Qi,⁴ G. Rong,⁴ P. Wang,⁴ Y. S. Zhu,⁴ G. Eigen,⁵
I. Ofte,⁵ B. Stugu,⁵ G. S. Abrams,⁶ M. Battaglia,⁶ D. N. Brown,⁶ J. Button-Shafer,⁶ R. N. Cahn,⁶ E. Charles,⁶
M. S. Gill,⁶ Y. Groysman,⁶ R. G. Jacobsen,⁶ J. A. Kadyk,⁶ L. T. Kerth,⁶ Yu. G. Kolomensky,⁶ G. Kukartsev,⁶
G. Lynch,⁶ L. M. Mir,⁶ T. J. Orimoto,⁶ M. Pripstein,⁶ N. A. Roe,⁶ M. T. Ronan,⁶ W. A. Wenzel,⁶
P. del Amo Sanchez,⁷ M. Barrett,⁷ K. E. Ford,⁷ T. J. Harrison,⁷ A. J. Hart,⁷ C. M. Hawkes,⁷ A. T. Watson,⁷
T. Held,⁸ H. Koch,⁸ B. Lewandowski,⁸ M. Pelizaeus,⁸ K. Peters,⁸ T. Schroeder,⁸ M. Steinke,⁸ J. T. Boyd,⁹
J. P. Burke,⁹ W. N. Cottingham,⁹ D. Walker,⁹ D. J. Asgeirsson,¹⁰ T. Cuhadar-Donszelmann,¹⁰ B. G. Fulsom,¹⁰
C. Hearty,¹⁰ N. S. Knecht,¹⁰ T. S. Mattison,¹⁰ J. A. McKenna,¹⁰ A. Khan,¹¹ P. Kyberd,¹¹ M. Saleem,¹¹
D. J. Sherwood,¹¹ L. Teodorescu,¹¹ V. E. Blinov,¹² A. D. Bukin,¹² V. P. Druzhinin,¹² V. B. Golubev,¹²
A. P. Onuchin,¹² S. I. Serednyakov,¹² Yu. I. Skovpen,¹² E. P. Solodov,¹² K. Yu Todyshev,¹² D. S. Best,¹³
M. Bondioli,¹³ M. Bruinsma,¹³ M. Chao,¹³ S. Curry,¹³ I. Eschrich,¹³ D. Kirkby,¹³ A. J. Lankford,¹³ P. Lund,¹³
M. Mandelkern,¹³ W. Roethel,¹³ D. P. Stoker,¹³ S. Abachi,¹⁴ C. Buchanan,¹⁴ S. D. Foulkes,¹⁵ J. W. Gary,¹⁵
O. Long,¹⁵ B. C. Shen,¹⁵ K. Wang,¹⁵ L. Zhang,¹⁵ H. K. Hadavand,¹⁶ E. J. Hill,¹⁶ H. P. Paar,¹⁶ S. Rahatlou,¹⁶
V. Sharma,¹⁶ J. W. Berryhill,¹⁷ C. Campagnari,¹⁷ A. Cunha,¹⁷ B. Dahmes,¹⁷ T. M. Hong,¹⁷ D. Kovalskyi,¹⁷
J. D. Richman,¹⁷ T. W. Beck,¹⁸ A. M. Eisner,¹⁸ C. J. Flacco,¹⁸ C. A. Heusch,¹⁸ J. Kroseberg,¹⁸ W. S. Lockman,¹⁸
G. Nesom,¹⁸ T. Schalk,¹⁸ B. A. Schumm,¹⁸ A. Seiden,¹⁸ P. Spradlin,¹⁸ D. C. Williams,¹⁸ M. G. Wilson,¹⁸
J. Albert,¹⁹ E. Chen,¹⁹ C. H. Cheng,¹⁹ A. Dvoretzki,¹⁹ F. Fang,¹⁹ D. G. Hitlin,¹⁹ I. Narsky,¹⁹ T. Piatenko,¹⁹
F. C. Porter,¹⁹ G. Mancinelli,²⁰ B. T. Meadows,²⁰ K. Mishra,²⁰ M. D. Sokoloff,²⁰ F. Blanc,²¹ P. C. Bloom,²¹
S. Chen,²¹ W. T. Ford,²¹ J. F. Hirschauer,²¹ A. Kreisel,²¹ M. Nagel,²¹ U. Nauenberg,²¹ A. Olivas,²¹
W. O. Ruddick,²¹ J. G. Smith,²¹ K. A. Ulmer,²¹ S. R. Wagner,²¹ J. Zhang,²¹ A. Chen,²² E. A. Eckhart,²²
A. Soffer,²² W. H. Toki,²² R. J. Wilson,²² F. Winklmeier,²² Q. Zeng,²² D. D. Altenburg,²³ E. Feltresi,²³ A. Hauke,²³
H. Jasper,²³ J. Merkel,²³ A. Petzold,²³ B. Spaan,²³ T. Brandt,²⁴ V. Klose,²⁴ H. M. Lacker,²⁴ W. F. Mader,²⁴
R. Nogowski,²⁴ J. Schubert,²⁴ K. R. Schubert,²⁴ R. Schwierz,²⁴ J. E. Sundermann,²⁴ A. Volk,²⁴ D. Bernard,²⁵
G. R. Bonneaud,²⁵ E. Latour,²⁵ Ch. Thiebaux,²⁵ M. Verderi,²⁵ P. J. Clark,²⁶ W. Gradl,²⁶ F. Muheim,²⁶
S. Playfer,²⁶ A. I. Robertson,²⁶ Y. Xie,²⁶ M. Andreotti,²⁷ D. Bettoni,²⁷ C. Bozzi,²⁷ R. Calabrese,²⁷ G. Cibinetto,²⁷
E. Luppi,²⁷ M. Negrini,²⁷ A. Petrella,²⁷ L. Piemontese,²⁷ E. Prencipe,²⁷ F. Anulli,²⁸ R. Baldini-Ferrolli,²⁸
A. Calcaterra,²⁸ R. de Sangro,²⁸ G. Finocchiaro,²⁸ S. Pacetti,²⁸ P. Patteri,²⁸ I. M. Peruzzi,²⁸ * M. Piccolo,²⁸
M. Rama,²⁸ A. Zallo,²⁸ A. Buzzo,²⁹ R. Contri,²⁹ M. Lo Vetere,²⁹ M. M. Macri,²⁹ M. R. Monge,²⁹ S. Passaggio,²⁹
C. Patrignani,²⁹ E. Robutti,²⁹ A. Santroni,²⁹ S. Tosi,²⁹ G. Brandenburg,³⁰ K. S. Chaisanguanthum,³⁰ M. Morii,³⁰
J. Wu,³⁰ R. S. Dubitzky,³¹ J. Marks,³¹ S. Schenk,³¹ U. Uwer,³¹ D. J. Bard,³² W. Bhimji,³² D. A. Bowerman,³²
P. D. Dauncey,³² U. Egede,³² R. L. Flack,³² J. A. Nash,³² M. B. Nikolich,³² W. Panduro Vazquez,³² P. K. Behera,³³
X. Chai,³³ M. J. Charles,³³ U. Mallik,³³ N. T. Meyer,³³ V. Ziegler,³³ J. Cochran,³⁴ H. B. Crawley,³⁴ L. Dong,³⁴
V. Eyges,³⁴ W. T. Meyer,³⁴ S. Prell,³⁴ E. I. Rosenberg,³⁴ A. E. Rubin,³⁴ A. V. Gritsan,³⁵ A. G. Denig,³⁶
M. Fritsch,³⁶ G. Schott,³⁶ N. Arnaud,³⁷ M. Davier,³⁷ G. Grosdidier,³⁷ A. Höcker,³⁷ F. Le Diberder,³⁷
V. Lepeltier,³⁷ A. M. Lutz,³⁷ A. Oyanguren,³⁷ S. Pruvot,³⁷ S. Rodier,³⁷ P. Roudeau,³⁷ M. H. Schune,³⁷
A. Stocchi,³⁷ W. F. Wang,³⁷ G. Wormser,³⁷ D. J. Lange,³⁸ D. M. Wright,³⁸ C. A. Chavez,³⁹ I. J. Forster,³⁹
J. R. Fry,³⁹ E. Gabathuler,³⁹ R. Gamet,³⁹ K. A. George,³⁹ D. E. Hutchcroft,³⁹ D. J. Payne,³⁹ K. C. Schofield,³⁹
C. Touramanis,³⁹ A. J. Bevan,⁴⁰ F. Di Lodovico,⁴⁰ W. Menges,⁴⁰ R. Sacco,⁴⁰ G. Cowan,⁴¹ H. U. Flaecher,⁴¹
D. A. Hopkins,⁴¹ P. S. Jackson,⁴¹ T. R. McMahon,⁴¹ F. Salvatore,⁴¹ A. C. Wren,⁴¹ D. N. Brown,⁴² C. L. Davis,⁴²
J. Allison,⁴³ N. R. Barlow,⁴³ R. J. Barlow,⁴³ Y. M. Chia,⁴³ C. L. Edgar,⁴³ G. D. Lafferty,⁴³ M. T. Naisbit,⁴³
J. C. Williams,⁴³ J. I. Yi,⁴³ C. Chen,⁴⁴ W. D. Hulsbergen,⁴⁴ A. Jawahery,⁴⁴ C. K. Lae,⁴⁴ D. A. Roberts,⁴⁴
G. Simi,⁴⁴ G. Blaylock,⁴⁵ C. Dallapiccola,⁴⁵ S. S. Hertzbach,⁴⁵ X. Li,⁴⁵ T. B. Moore,⁴⁵ S. Saremi,⁴⁵ H. Staengle,⁴⁵
R. Cowan,⁴⁶ G. Sciolla,⁴⁶ S. J. Sekula,⁴⁶ M. Spitznagel,⁴⁶ F. Taylor,⁴⁶ R. K. Yamamoto,⁴⁶ H. Kim,⁴⁷
S. E. Mclachlin,⁴⁷ P. M. Patel,⁴⁷ S. H. Robertson,⁴⁷ A. Lazzaro,⁴⁸ V. Lombardo,⁴⁸ F. Palombo,⁴⁸ J. M. Bauer,⁴⁹
L. Cremaldi,⁴⁹ V. Eschenburg,⁴⁹ R. Godang,⁴⁹ R. Kroeger,⁴⁹ D. A. Sanders,⁴⁹ D. J. Summers,⁴⁹ H. W. Zhao,⁴⁹
S. Brunet,⁵⁰ D. Côté,⁵⁰ M. Simard,⁵⁰ P. Taras,⁵⁰ F. B. Viaud,⁵⁰ H. Nicholson,⁵¹ N. Cavallo,⁵² † G. De Nardo,⁵²
F. Fabozzi,⁵² † C. Gatto,⁵² L. Lista,⁵² D. Monorchio,⁵² P. Paolucci,⁵² D. Piccolo,⁵² C. Sciacca,⁵² M. A. Baak,⁵³
G. Raven,⁵³ H. L. Snoek,⁵³ C. P. Jessop,⁵⁴ J. M. LoSecco,⁵⁴ G. Benelli,⁵⁵ L. A. Corwin,⁵⁵ K. K. Gan,⁵⁵
K. Honscheid,⁵⁵ D. Hufnagel,⁵⁵ P. D. Jackson,⁵⁵ H. Kagan,⁵⁵ R. Kass,⁵⁵ A. M. Rahimi,⁵⁵ J. J. Regensburger,⁵⁵

R. Ter-Antonyan,⁵⁵ Q. K. Wong,⁵⁵ N. L. Blount,⁵⁶ J. Brau,⁵⁶ R. Frey,⁵⁶ O. Igonkina,⁵⁶ J. A. Kolb,⁵⁶ M. Lu,⁵⁶ R. Rahmat,⁵⁶ N. B. Sinev,⁵⁶ D. Strom,⁵⁶ J. Strube,⁵⁶ E. Torrence,⁵⁶ A. Gaz,⁵⁷ M. Margoni,⁵⁷ M. Morandin,⁵⁷ A. Pompili,⁵⁷ M. Posocco,⁵⁷ M. Rotondo,⁵⁷ F. Simonetto,⁵⁷ R. Stroili,⁵⁷ C. Voci,⁵⁷ M. Benayoun,⁵⁸ H. Briand,⁵⁸ J. Chauveau,⁵⁸ P. David,⁵⁸ L. Del Buono,⁵⁸ Ch. de la Vaissière,⁵⁸ O. Hamon,⁵⁸ B. L. Hartfiel,⁵⁸ Ph. Leruste,⁵⁸ J. Malclès,⁵⁸ J. Ocariz,⁵⁸ L. Roos,⁵⁸ G. Therin,⁵⁸ L. Gladney,⁵⁹ M. Biasini,⁶⁰ R. Covarelli,⁶⁰ C. Angelini,⁶¹ G. Batignani,⁶¹ S. Bettarini,⁶¹ F. Bucci,⁶¹ G. Calderini,⁶¹ M. Carpinelli,⁶¹ R. Cenci,⁶¹ F. Forti,⁶¹ M. A. Giorgi,⁶¹ A. Lusiani,⁶¹ G. Marchiori,⁶¹ M. A. Mazur,⁶¹ M. Morganti,⁶¹ N. Neri,⁶¹ E. Paoloni,⁶¹ G. Rizzo,⁶¹ J. J. Walsh,⁶¹ M. Haire,⁶² D. Judd,⁶² D. E. Wagoner,⁶² J. Biesiada,⁶³ N. Danielson,⁶³ P. Elmer,⁶³ Y. P. Lau,⁶³ C. Lu,⁶³ J. Olsen,⁶³ A. J. S. Smith,⁶³ A. V. Telnov,⁶³ F. Bellini,⁶⁴ G. Cavoto,⁶⁴ A. D’Orazio,⁶⁴ D. del Re,⁶⁴ E. Di Marco,⁶⁴ R. Faccini,⁶⁴ F. Ferrarotto,⁶⁴ F. Ferroni,⁶⁴ M. Gaspero,⁶⁴ L. Li Gioi,⁶⁴ M. A. Mazzoni,⁶⁴ S. Morganti,⁶⁴ G. Piredda,⁶⁴ F. Polci,⁶⁴ F. Safai Tehrani,⁶⁴ C. Voena,⁶⁴ M. Ebert,⁶⁵ H. Schröder,⁶⁵ R. Waldi,⁶⁵ T. Adye,⁶⁶ B. Franek,⁶⁶ E. O. Olaiya,⁶⁶ S. Ricciardi,⁶⁶ F. F. Wilson,⁶⁶ R. Aleksan,⁶⁷ S. Emery,⁶⁷ A. Gaidot,⁶⁷ S. F. Ganzhur,⁶⁷ G. Hamel de Monchenault,⁶⁷ W. Kozanecki,⁶⁷ M. Legendre,⁶⁷ G. Vasseur,⁶⁷ Ch. Yèche,⁶⁷ M. Zito,⁶⁷ X. R. Chen,⁶⁸ H. Liu,⁶⁸ W. Park,⁶⁸ M. V. Purohit,⁶⁸ J. R. Wilson,⁶⁸ M. T. Allen,⁶⁹ D. Aston,⁶⁹ R. Bartoldus,⁶⁹ P. Bechtel,⁶⁹ N. Berger,⁶⁹ R. Claus,⁶⁹ J. P. Coleman,⁶⁹ M. R. Convery,⁶⁹ J. C. Dingfelder,⁶⁹ J. Dorfan,⁶⁹ G. P. Dubois-Felsmann,⁶⁹ D. Dujmic,⁶⁹ W. Dunwoodie,⁶⁹ R. C. Field,⁶⁹ T. Glanzman,⁶⁹ S. J. Gowdy,⁶⁹ M. T. Graham,⁶⁹ P. Grenier,⁶⁹ V. Halyo,⁶⁹ C. Hast,⁶⁹ T. Hryn’ova,⁶⁹ W. R. Innes,⁶⁹ M. H. Kelsey,⁶⁹ P. Kim,⁶⁹ D. W. G. S. Leith,⁶⁹ S. Li,⁶⁹ S. Luitz,⁶⁹ V. Luth,⁶⁹ H. L. Lynch,⁶⁹ D. B. MacFarlane,⁶⁹ H. Marsiske,⁶⁹ R. Messner,⁶⁹ D. R. Muller,⁶⁹ C. P. O’Grady,⁶⁹ V. E. Ozcan,⁶⁹ A. Perazzo,⁶⁹ M. Perl,⁶⁹ T. Pulliam,⁶⁹ B. N. Ratcliff,⁶⁹ A. Roodman,⁶⁹ A. A. Salmikov,⁶⁹ R. H. Schindler,⁶⁹ J. Schwiening,⁶⁹ A. Snyder,⁶⁹ J. Stelzer,⁶⁹ D. Su,⁶⁹ M. K. Sullivan,⁶⁹ K. Suzuki,⁶⁹ S. K. Swain,⁶⁹ J. M. Thompson,⁶⁹ J. Va’vra,⁶⁹ N. van Bakel,⁶⁹ M. Weaver,⁶⁹ A. J. R. Weinstein,⁶⁹ W. J. Wisniewski,⁶⁹ M. Wittgen,⁶⁹ D. H. Wright,⁶⁹ A. K. Yarritu,⁶⁹ K. Yi,⁶⁹ C. C. Young,⁶⁹ P. R. Burchat,⁷⁰ A. J. Edwards,⁷⁰ S. A. Majewski,⁷⁰ B. A. Petersen,⁷⁰ L. Wilden,⁷⁰ S. Ahmed,⁷¹ M. S. Alam,⁷¹ R. Bula,⁷¹ J. A. Ernst,⁷¹ V. Jain,⁷¹ B. Pan,⁷¹ M. A. Saeed,⁷¹ F. R. Wappler,⁷¹ S. B. Zain,⁷¹ W. Bugg,⁷² M. Krishnamurthy,⁷² S. M. Spanier,⁷² R. Eckmann,⁷³ J. L. Ritchie,⁷³ A. Satpathy,⁷³ C. J. Schilling,⁷³ R. F. Schwitters,⁷³ J. M. Izen,⁷⁴ X. C. Lou,⁷⁴ S. Ye,⁷⁴ F. Bianchi,⁷⁵ F. Gallo,⁷⁵ D. Gamba,⁷⁵ M. Bomben,⁷⁶ L. Bosisio,⁷⁶ C. Cartaro,⁷⁶ F. Cossutti,⁷⁶ G. Della Ricca,⁷⁶ S. Dittongo,⁷⁶ L. Lanceri,⁷⁶ L. Vitale,⁷⁶ V. Azzolini,⁷⁷ N. Lopez-March,⁷⁷ F. Martinez-Vidal,⁷⁷ Sw. Banerjee,⁷⁸ B. Bhuyan,⁷⁸ C. M. Brown,⁷⁸ D. Fortin,⁷⁸ K. Hamano,⁷⁸ R. Kowalewski,⁷⁸ I. M. Nugent,⁷⁸ J. M. Roney,⁷⁸ R. J. Sobie,⁷⁸ J. J. Back,⁷⁹ P. F. Harrison,⁷⁹ T. E. Latham,⁷⁹ G. B. Mohanty,⁷⁹ M. Pappagallo,⁷⁹ † H. R. Band,⁸⁰ X. Chen,⁸⁰ B. Cheng,⁸⁰ S. Dasu,⁸⁰ M. Datta,⁸⁰ K. T. Flood,⁸⁰ J. J. Hollar,⁸⁰ P. E. Kutter,⁸⁰ B. Mellado,⁸⁰ A. Mihalyi,⁸⁰ Y. Pan,⁸⁰ M. Pierini,⁸⁰ R. Prepost,⁸⁰ S. L. Wu,⁸⁰ Z. Yu,⁸⁰ and H. Neal⁸¹

(The BABAR Collaboration)

¹Laboratoire de Physique des Particules, IN2P3/CNRS et Université de Savoie, F-74941 Annecy-Le-Vieux, France

²Universitat de Barcelona, Facultat de Física, Departament ECM, E-08028 Barcelona, Spain

³Università di Bari, Dipartimento di Fisica and INFN, I-70126 Bari, Italy

⁴Institute of High Energy Physics, Beijing 100039, China

⁵University of Bergen, Institute of Physics, N-5007 Bergen, Norway

⁶Lawrence Berkeley National Laboratory and University of California, Berkeley, California 94720, USA

⁷University of Birmingham, Birmingham, B15 2TT, United Kingdom

⁸Ruhr Universität Bochum, Institut für Experimentalphysik 1, D-44780 Bochum, Germany

⁹University of Bristol, Bristol BS8 1TL, United Kingdom

¹⁰University of British Columbia, Vancouver, British Columbia, Canada V6T 1Z1

¹¹Brunel University, Uxbridge, Middlesex UB8 3PH, United Kingdom

¹²Budker Institute of Nuclear Physics, Novosibirsk 630090, Russia

¹³University of California at Irvine, Irvine, California 92697, USA

¹⁴University of California at Los Angeles, Los Angeles, California 90024, USA

¹⁵University of California at Riverside, Riverside, California 92521, USA

¹⁶University of California at San Diego, La Jolla, California 92093, USA

¹⁷University of California at Santa Barbara, Santa Barbara, California 93106, USA

¹⁸University of California at Santa Cruz, Institute for Particle Physics, Santa Cruz, California 95064, USA

¹⁹California Institute of Technology, Pasadena, California 91125, USA

²⁰University of Cincinnati, Cincinnati, Ohio 45221, USA

²¹University of Colorado, Boulder, Colorado 80309, USA

²²Colorado State University, Fort Collins, Colorado 80523, USA

²³Universität Dortmund, Institut für Physik, D-44221 Dortmund, Germany

²⁴Technische Universität Dresden, Institut für Kern- und Teilchenphysik, D-01062 Dresden, Germany

²⁵Laboratoire Leprince-Ringuet, CNRS/IN2P3, Ecole Polytechnique, F-91128 Palaiseau, France

- ²⁶University of Edinburgh, Edinburgh EH9 3JZ, United Kingdom
- ²⁷Università di Ferrara, Dipartimento di Fisica and INFN, I-44100 Ferrara, Italy
- ²⁸Laboratori Nazionali di Frascati dell'INFN, I-00044 Frascati, Italy
- ²⁹Università di Genova, Dipartimento di Fisica and INFN, I-16146 Genova, Italy
- ³⁰Harvard University, Cambridge, Massachusetts 02138, USA
- ³¹Universität Heidelberg, Physikalisches Institut, Philosophenweg 12, D-69120 Heidelberg, Germany
- ³²Imperial College London, London, SW7 2AZ, United Kingdom
- ³³University of Iowa, Iowa City, Iowa 52242, USA
- ³⁴Iowa State University, Ames, Iowa 50011-3160, USA
- ³⁵Johns Hopkins University, Baltimore, Maryland 21218, USA
- ³⁶Universität Karlsruhe, Institut für Experimentelle Kernphysik, D-76021 Karlsruhe, Germany
- ³⁷Laboratoire de l'Accélérateur Linéaire, IN2P3/CNRS et Université Paris-Sud 11, Centre Scientifique d'Orsay, B.P. 34, F-91898 ORSAY Cedex, France
- ³⁸Lawrence Livermore National Laboratory, Livermore, California 94550, USA
- ³⁹University of Liverpool, Liverpool L69 7ZE, United Kingdom
- ⁴⁰Queen Mary, University of London, E1 4NS, United Kingdom
- ⁴¹University of London, Royal Holloway and Bedford New College, Egham, Surrey TW20 0EX, United Kingdom
- ⁴²University of Louisville, Louisville, Kentucky 40292, USA
- ⁴³University of Manchester, Manchester M13 9PL, United Kingdom
- ⁴⁴University of Maryland, College Park, Maryland 20742, USA
- ⁴⁵University of Massachusetts, Amherst, Massachusetts 01003, USA
- ⁴⁶Massachusetts Institute of Technology, Laboratory for Nuclear Science, Cambridge, Massachusetts 02139, USA
- ⁴⁷McGill University, Montréal, Québec, Canada H3A 2T8
- ⁴⁸Università di Milano, Dipartimento di Fisica and INFN, I-20133 Milano, Italy
- ⁴⁹University of Mississippi, University, Mississippi 38677, USA
- ⁵⁰Université de Montréal, Physique des Particules, Montréal, Québec, Canada H3C 3J7
- ⁵¹Mount Holyoke College, South Hadley, Massachusetts 01075, USA
- ⁵²Università di Napoli Federico II, Dipartimento di Scienze Fisiche and INFN, I-80126, Napoli, Italy
- ⁵³NIKHEF, National Institute for Nuclear Physics and High Energy Physics, NL-1009 DB Amsterdam, The Netherlands
- ⁵⁴University of Notre Dame, Notre Dame, Indiana 46556, USA
- ⁵⁵Ohio State University, Columbus, Ohio 43210, USA
- ⁵⁶University of Oregon, Eugene, Oregon 97403, USA
- ⁵⁷Università di Padova, Dipartimento di Fisica and INFN, I-35131 Padova, Italy
- ⁵⁸Laboratoire de Physique Nucléaire et de Hautes Energies, IN2P3/CNRS, Université Pierre et Marie Curie-Paris6, Université Denis Diderot-Paris7, F-75252 Paris, France
- ⁵⁹University of Pennsylvania, Philadelphia, Pennsylvania 19104, USA
- ⁶⁰Università di Perugia, Dipartimento di Fisica and INFN, I-06100 Perugia, Italy
- ⁶¹Università di Pisa, Dipartimento di Fisica, Scuola Normale Superiore and INFN, I-56127 Pisa, Italy
- ⁶²Prairie View A&M University, Prairie View, Texas 77446, USA
- ⁶³Princeton University, Princeton, New Jersey 08544, USA
- ⁶⁴Università di Roma La Sapienza, Dipartimento di Fisica and INFN, I-00185 Roma, Italy
- ⁶⁵Universität Rostock, D-18051 Rostock, Germany
- ⁶⁶Rutherford Appleton Laboratory, Chilton, Didcot, Oxon, OX11 0QX, United Kingdom
- ⁶⁷DSM/Dapnia, CEA/Saclay, F-91191 Gif-sur-Yvette, France
- ⁶⁸University of South Carolina, Columbia, South Carolina 29208, USA
- ⁶⁹Stanford Linear Accelerator Center, Stanford, California 94309, USA
- ⁷⁰Stanford University, Stanford, California 94305-4060, USA
- ⁷¹State University of New York, Albany, New York 12222, USA
- ⁷²University of Tennessee, Knoxville, Tennessee 37996, USA
- ⁷³University of Texas at Austin, Austin, Texas 78712, USA
- ⁷⁴University of Texas at Dallas, Richardson, Texas 75083, USA
- ⁷⁵Università di Torino, Dipartimento di Fisica Sperimentale and INFN, I-10125 Torino, Italy
- ⁷⁶Università di Trieste, Dipartimento di Fisica and INFN, I-34127 Trieste, Italy
- ⁷⁷IFIC, Universitat de Valencia-CSIC, E-46071 Valencia, Spain
- ⁷⁸University of Victoria, Victoria, British Columbia, Canada V8W 3P6
- ⁷⁹Department of Physics, University of Warwick, Coventry CV4 7AL, United Kingdom
- ⁸⁰University of Wisconsin, Madison, Wisconsin 53706, USA
- ⁸¹Yale University, New Haven, Connecticut 06511, USA

(Dated: October 1, 2018)

We present improved measurements of the branching fraction and CP asymmetry for the process $B^\pm \rightarrow \rho^\pm \pi^0$. The data sample corresponding to 211 fb^{-1} comprises 232 million $\Upsilon(4S) \rightarrow B\bar{B}$ decays collected with the BABAR detector at the PEP-II asymmetric B Factory at SLAC. The yield and

CP asymmetry are measured using an extended maximum likelihood fitting method. The branching fraction and CP asymmetry are found to be $\mathcal{B}(B^\pm \rightarrow \rho^\pm \pi^0) = [10.2 \pm 1.4 \text{ (stat)} \pm 0.9 \text{ (syst)}] \times 10^{-6}$ and $\mathcal{A}_{CP}(B^\pm \rightarrow \rho^\pm \pi^0) = -0.01 \pm 0.13 \text{ (stat)} \pm 0.02 \text{ (syst)}$.

PACS numbers: 11.30.Er, 13.25.Hw

Branching fraction and CP asymmetry measurements of charmless B meson decays provide valuable constraints for the determination of the unitarity triangle constructed from elements of the Cabibbo-Kobayashi-Maskawa quark-mixing matrix [1, 2]. In particular, the angle $\alpha \equiv \arg[-V_{td}V_{tb}^*/V_{ud}V_{ub}^*]$ of the Unitarity Triangle can be extracted from decays of the B meson to $\rho^\pm \pi^\mp$ final states [3]. However, the extraction is complicated by the interference of decay amplitudes with differing weak and strong phases. One strategy to overcome this problem is to perform an $SU(2)$ analysis that uses all $\rho\pi$ final states [4]. Assuming isospin symmetry, the angle α can be determined free of hadronic uncertainties from a pentagon relation formed in the complex plane by the five $B \rightarrow \rho\pi$ decay amplitudes $B^0 \rightarrow \rho^+\pi^-$, $B^0 \rightarrow \rho^-\pi^+$, $B^0 \rightarrow \rho^0\pi^0$, $B^+ \rightarrow \rho^+\pi^0$ and $B^+ \rightarrow \rho^0\pi^+$. These amplitudes can be determined from measurements of the corresponding decay rates and CP asymmetries. While all these modes have been measured [5, 6], the current experimental uncertainties need to be reduced substantially for a determination of α . Here we present an update to previous measurements of the $B^\pm \rightarrow \rho^\pm \pi^0$ branching fraction and CP asymmetry

$$\mathcal{A}_{CP} = \frac{N(B^- \rightarrow \rho^- \pi^0) - N(B^+ \rightarrow \rho^+ \pi^0)}{N(B^- \rightarrow \rho^- \pi^0) + N(B^+ \rightarrow \rho^+ \pi^0)}.$$

The main additions compared to our previous analysis [5] are a larger dataset, a study of possible backgrounds from higher ρ resonances and the use of the ρ mass in the maximum likelihood fit.

The data were collected with the *BABAR* detector [7] at the PEP-II asymmetric-energy e^+e^- storage ring at SLAC. Charged-particle trajectories are measured by a five-layer double-sided silicon vertex tracker and a 40-layer drift chamber located within a 1.5-T magnetic field. Charged hadrons are identified by combining energy-loss information from tracking (dE/dx) with the measurements from a ring-imaging Cherenkov detector. Photons are detected by a CsI(Tl) crystal electromagnetic calorimeter with an energy resolution of $\sigma_E/E = 0.023(E/\text{GeV})^{-1/4} \oplus 0.014$. The magnetic flux return is instrumented for muon and K_L^0 identification. The data sample includes 232 ± 3 million $B\bar{B}$ pairs collected at the $\Upsilon(4S)$ resonance, corresponding to an integrated luminosity of 211 fb^{-1} . In addition, 22 fb^{-1} of

data collected 40 MeV below the $\Upsilon(4S)$ resonance mass are used for background studies. We perform full detector Monte Carlo (MC) simulations equivalent to 460 fb^{-1} of generic $B\bar{B}$ decays and 140 fb^{-1} of continuum quark-antiquark events ($e^+e^- \rightarrow q\bar{q}$, $q = u, d, s, c$). In addition, we simulate over 50 exclusive charmless B meson decay modes, including 1.4 million signal $B^\pm \rightarrow \rho^\pm \pi^0$ decays.

B meson candidates are reconstructed from one charged track and two neutral pions. The charged track used to form the $B^\pm \rightarrow \rho^\pm \pi^0$ candidate is required to have at least 12 hits in the drift chamber, to have a transverse momentum greater than $0.1 \text{ GeV}/c$, and to be consistent with originating from the beam-spot. It must have ionization-energy loss and Cherenkov angle signatures consistent with those expected for a pion. We remove charged tracks that pass electron selection criteria based on dE/dx and calorimeter information. Neutral pion candidates are formed from two photon candidates, each with a minimum energy of 0.03 GeV and which are required to exhibit a lateral profile of energy deposition in the electromagnetic calorimeter consistent with an electromagnetic shower [7]. The angular acceptance of photon candidates is restricted to exclude parts of the calorimeter where showers are not fully contained. We require the photon clusters forming the π^0 to be separated in space, with a π^0 energy of at least 0.2 GeV and an invariant mass between 0.10 and $0.16 \text{ GeV}/c^2$.

Two kinematic variables, $\Delta E = E_B^* - \sqrt{s}/2$ and the beam-energy substituted mass of the B meson $m_{ES} = \sqrt{(s/2 + \mathbf{p}_0 \cdot \mathbf{p}_B)^2/E_0^2 - \mathbf{p}_B^2}$, are used for the final selection of events. Here E_B^* is the energy of the B meson candidate in the center-of-mass frame, E_0 and \sqrt{s} are the total energies of the e^+e^- system in the laboratory and center-of-mass frames, respectively; and \mathbf{p}_0 and \mathbf{p}_B are the three-momenta of the e^+e^- system and the B meson candidate in the laboratory frame, respectively. For correctly reconstructed $\rho^\pm \pi^0$ candidates ΔE peaks at zero, while for final states with a charged kaon, such as $B^\pm \rightarrow K^{*\pm} \pi^0$, ΔE is shifted by approximately 80 MeV on average. Events are selected with $5.20 < m_{ES} < 5.29 \text{ GeV}/c^2$ and $|\Delta E| < 0.20 \text{ GeV}$. The ΔE limits remove background from two- and four-body B meson decays with a small loss in signal efficiency.

Continuum events are the dominant background. To suppress this background, we select only those events where the angle θ_{Sph}^B in the center-of-mass frame between the sphericity axis [8] of the B meson candidate's decay products and the sphericity axis of the rest of the event satisfies $|\cos \theta_{\text{Sph}}^B| < 0.9$. In addition, we construct a non-linear discriminant, implemented as an artificial neural network (A_{NN}) that uses three input parameters: the zeroth- and second-order Legendre event shape polyno-

*Also with Università di Perugia, Dipartimento di Fisica, Perugia, Italy

†Also with Università della Basilicata, Potenza, Italy

‡Also with IPPP, Physics Department, Durham University, Durham DH1 3LE, United Kingdom

mials L_0 and L_2 calculated from the momenta and polar angles, with respect to the B meson thrust axis, of all charged particle and photon candidates not associated with the B meson candidate, and the output of a multivariate, non-linear B meson candidate flavor tagging algorithm [9]. The output A_{NN} of the artificial neural network peaks at 0.5 for continuum-like events and at 1.0 for B meson decays. We require $A_{\text{NN}} > 0.63$ which reduces the continuum background by half for a 5% loss in signal MC efficiency. To further improve the signal-to-background ratio we restrict the invariant mass of the ρ candidate to $0.55 < m_{\pi\pi} < 0.95 \text{ GeV}/c^2$.

The average B meson candidate multiplicity per event is 1.8 as neutral and charged pion combinatorics can lead to more than one B meson candidate. We choose the best candidate based on a χ^2 formed from the measured masses of the two π^0 candidates within the event compared to the known π^0 mass [10]. In the case of multiple charged pion candidates the choice is random so as not to bias the fit distributions. This random selection has a negligible impact on the systematic uncertainty. The total $B^\pm \rightarrow \rho^\pm \pi^0$ selection efficiency is $15.4 \pm 0.1\%$. In signal MC studies, the candidate is correctly reconstructed 54.9% of the time. The remaining candidates come from self-cross-feed (SCF, 37.5%) and mistag events (7.6%). SCF events stem primarily from swapping the low energy π^0 from the resonance with another from the rest of the event. Signal events reconstructed with the wrong charge are classified as mistag events. Both SCF and mistag events emulate signal events, however the resolution in m_{ES} and ΔE tends to be worse.

We use MC events to study the backgrounds from other B -meson decays. The dominant contribution comes from $b \rightarrow c$ transitions; the next most important is from charmless B -meson decays. Seventeen individual charmless modes show a significant contribution once the event selection has been applied. These modes are added into the fit (described below) fixed at the yield and asymmetry determined by the simulation, based on their measured values [10]. The largest contributions come from $B^0 \rightarrow \rho^\pm \rho^\mp$ and $B^0 \rightarrow \rho^\pm \pi^\mp$. For $B^0 \rightarrow \eta' \pi^0$ and $B^0 \rightarrow K^{*\pm} \rho^\mp$ we use half the measured upper limit [10]. We estimate the $B^0 \rightarrow a_1^0 \pi^0$ branching fraction from that of $B^0 \rightarrow a_1^+ \pi^-$ [11] using isospin relations. If no charge asymmetry measurement is available, we assume zero asymmetry.

Although all other states that decay like the ρ to $\pi\pi^0$ – the $\rho(1450)$ and the $\rho(1700)$, subsequently referred to collectively as ρ^* – lie outside our $\rho(770)$ mass cut, a contribution to our signal cannot be ruled out *a priori*. To account for the possible presence of these modes, an unbinned maximum likelihood fit to the $B^\pm \rightarrow \rho^{*\pm} \pi^0$ yield is performed in a sideband of the $m_{\pi\pi}$ invariant mass. This fit uses the same algorithm as described below but with only the three input variables m_{ES} , ΔE , and A_{NN} . The mass window is chosen to be as far as possible from the $\rho(770)$ mass, centered near the pole of the $\rho(1700)$ at $1.5 < m_{\pi\pi} < 2.0 \text{ GeV}/c^2$. The fitted

yield for the $B^\pm \rightarrow \rho^{*\pm} \pi^0$ decay is then extrapolated into the $\rho(770)$ region, $0.55 < m_{\pi\pi} < 0.95 \text{ GeV}/c^2$, using a non-relativistic Breit-Wigner line-shape. Although the choice of mass range is motivated by the $\rho(1700)$, any yield seen is attributed entirely to the $\rho(1450)$, which is the closer of the two resonances to the signal. From the $B^\pm \rightarrow \rho^\pm(1450)\pi^0$ MC, the ratio of the number of candidates in the sideband to candidates in the signal mass region is approximately 12.6:1. The fit in the sideband yields 101 ± 32 events, resulting in an estimate of the ρ^* background of 8 events. We investigate possible interference effects by using an analytical model for the line-shapes of the $\rho(770)$ and the ρ^* . We compare the use of relativistic and non-relativistic Breit Wigner lineshapes and vary the widths of the lineshapes by their uncertainties [10]. We also scan the relative phase between the two resonances from $-\pi$ to π . We assign a conservative systematic uncertainty of 100% for the ρ^* background based on the largest change in the number of events in the range $0.55 < m_{\pi\pi} < 0.95 \text{ GeV}/c^2$ from these tests. The ρ^* then enters into the nominal fit with PDFs constructed from $B^\pm \rightarrow \rho^\pm(1450)\pi^0$ MC simulation.

The non-resonant $B^\pm \rightarrow \pi^\pm \pi^0 \pi^0$ branching fraction has, to date, not been measured. To estimate the size of its contribution we select a region of the Dalitz plot — defined by the triangle $(m_{\pi^\pm \pi_1^0}^2, m_{\pi^\pm \pi_2^0}^2) = (6, 6), (6, 15), (11, 11) \text{ GeV}^2/c^4$ — that is far from the signal as well as the $\rho(1450)$ and higher resonances and which has low levels of continuum background. The unbinned maximum likelihood fit with only three input variables (m_{ES} , ΔE , and A_{NN}) is applied in this region. The only significant backgrounds expected are from generic B and continuum events. The yields of the generic B decays are fixed to values expected from MC simulation while the continuum and non-resonant yields are allowed to float. There are 1100 data events in the selected Dalitz region and the fit yields -5.1 ± 7.6 non-resonant events. This is consistent with zero and the non-resonant contribution is therefore not considered as a background to our signal.

An unbinned maximum likelihood fit to the variables m_{ES} , ΔE , A_{NN} and $m_{\pi\pi}$ is used to extract the total number of signal $B^\pm \rightarrow \rho^\pm \pi^0$ and continuum background events and their respective charge asymmetries. The likelihood for the selected sample is given by the product of the probability density functions (PDF) for each individual candidate, multiplied by the Poisson factor:

$$\mathcal{L} = \frac{1}{N!} e^{-N'} (N')^N \prod_{i=1}^N \mathcal{P}_i,$$

where N and N' are the number of observed and expected events, respectively. The PDF \mathcal{P}_i for a given event i is a

sum of the signal and background terms:

$$\begin{aligned} \mathcal{P}_i = & N^{\text{Sig}} \times \frac{1}{2} [(1 - Q_i A_i^{\text{Sig}}) f_{\text{Sig}} \mathcal{P}_i^{\text{Sig}} \\ & + (1 - Q_i A_i^{\text{Sig}}) f_{\text{SCF}} \mathcal{P}_{\text{SCF},i}^{\text{Sig}} \\ & + (1 + Q_i A_i^{\text{Sig}}) f_{\text{Mis}} \mathcal{P}_{\text{Mis},i}^{\text{Sig}}] \\ & + \sum_j N_j^{\text{Bkg}} \times \frac{1}{2} (1 - Q_i A_j^{\text{Bkg}}) \mathcal{P}_{j,i}^{\text{Bkg}}, \end{aligned}$$

where Q_i is the charge of the pion in the event, $N^{\text{Sig}}(N_j^{\text{Bkg}})$ and $A^{\text{Sig}}(A_j^{\text{Bkg}})$ are the yield and asymmetry for signal (background) component j , respectively. The fractions of true signal (f_{Sig}), SCF signal (f_{SCF}), and wrong-charge mistag events (f_{Mis}) are fixed to the numbers obtained from MC simulations. The j individual background terms comprise continuum, $b \rightarrow c$ decays, ρ^* , and seventeen other exclusive charmless B meson decay modes. Signal and continuum yields are allowed to float in the fit, with the generic B yields fixed to values expected from MC simulation. The PDF for each component, in turn, is the product of the PDFs for each of the fit input variables, $\mathcal{P} = \mathcal{P}(m_{\text{ES}}, \Delta E) \mathcal{P}(A_{\text{NN}}) \mathcal{P}(m_{\pi\pi})$. Due to correlations between ΔE and m_{ES} , the $\mathcal{P}(m_{\text{ES}}, \Delta E)$ for signal and all background from B meson decays are described by two-dimensional non-parametric PDFs [12] obtained from MC events. For continuum background, $\mathcal{P}(m_{\text{ES}}, \Delta E)$ is the product of two one-dimensional non-parametric PDFs; m_{ES} is well described by an empirical phase-space threshold function [13] and ΔE is parameterized with a second degree polynomial. The parameters of the continuum PDFs are allowed to float in the fit except for the endpoint of the empirical phase-space threshold function which is fixed at $5.29 \text{ GeV}/c^2$. A_{NN} is described by the product of an exponential and a polynomial function for continuum background and by a Gaussian with a power-law tail on one side [14] for all other modes. For $\mathcal{P}(m_{\pi\pi})$, one-dimensional non-parametric PDFs obtained from MC events are used to describe all modes except the signal mode itself, which is described by a non-relativistic Breit-Wigner line-shape. The parameters for this PDF are held fixed to the MC values and varied within errors to estimate systematic uncertainties.

A number of cross checks confirm that the fit is unbiased. Using a double Gaussian PDF instead of a Breit-Wigner or omitting $m_{\pi\pi}$ altogether as a fit variable has no significant effect on the measured branching fraction. In 1000 MC pseudo-experiments, we use the maximum likelihood fit to extract the yields and asymmetries. The distributions for each component are generated from the component's PDF, giving values for the fit variables m_{ES} , ΔE , A_{NN} and $m_{\pi\pi}$. The expected number of events is calculated from the branching fraction and efficiency for each individual mode. The generated number of events for each fit component is determined by varying the expected number according to a Poisson distribution. The test is repeated using samples with different asymmetry values. We repeat these MC studies using fully simu-

lated signal $B^\pm \rightarrow \rho^\pm \pi^0$ events instead of generating the signal component from the PDFs. This verifies that the signal component is correctly modeled, including correlations between the fit variables. As another cross check we compare the distribution of the helicity angle θ_{Hel} between the momenta of the charged pion and the B meson in the ρ rest frame in data with that modeled in MC samples for a variety of selection criteria. To investigate the possible effects of interference, we repeat the analysis excluding events where both $m_{\pi^\pm \pi^0}$ combinations were in the range 0.55 to 0.95 GeV/c^2 ; the branching fraction decreases by 0.1%. k

TABLE I: Summary of the systematic uncertainties.

Absolute uncertainties on yields	
Source	$\sigma_{\text{Syst.}}^{\text{Yield}}$ (Events)
B background normalization	+ 6.9 - 7.2
PDF shapes	+ 4.7 - 4.2
SCF fraction	± 12.2
Mistag fraction	± 2.0
ΔE shift	± 2.6
Total	± 15
Relative uncertainties on $\mathcal{B}(B^\pm \rightarrow \rho^\pm \pi^0)$	
Source	$\sigma_{\text{Syst.}}^{\mathcal{B}}$ (%)
Efficiency estimation	± 7.3
B counting	± 1.1
Total	± 7.4
Uncertainties on \mathcal{A}_{CP}	
Source	$\sigma_{\text{Syst.}}^{\mathcal{A}_{CP}}$
Background normalization	± 0.006
Background asymmetry	± 0.024
PDF shapes	± 0.001
Total	± 0.02

Individual contributions to the systematic uncertainty are summarized in Table I. For each contributing exclusive B meson decay mode, we vary the number of events in the fit by its measured uncertainty, or by $\pm 100\%$ if derived from an upper limit. For the $b \rightarrow c$ component, we fix the rate based on the number calculated from MC samples and vary the amount based on the statistical uncertainty on this number. The shifts in the fitted yields are calculated for each mode in turn and then added in quadrature to find the total systematic effect. To take into account the variation of the two-dimensional non-parametric PDFs used for ΔE and m_{ES} , we smear the MC-generated distributions from which the PDFs are derived. This is effectively done by varying the kernel bandwidth [12] up to twice its original value. For $m_{\pi\pi}$ and A_{NN} , the parameterizations determined from fits to MC events are varied by one standard deviation. The systematic uncertainties are determined using the altered PDFs

and fitting to the final data sample. The overall shifts in the central value are taken as the size of the systematic uncertainty. We vary the SCF fraction by a conservative estimate of its relative uncertainty ($\pm 10\%$) and assign the shift in the fitted number of signal events as the systematic uncertainty of the SCF fraction. To account for differences in the neutral particle reconstruction between data and MC simulation, the signal PDF distribution in ΔE is offset by ± 5 MeV and the data are then refit. The larger of the two shifts in the central value of the yield is 2.6 events, which is taken as the systematic uncertainty for this effect.

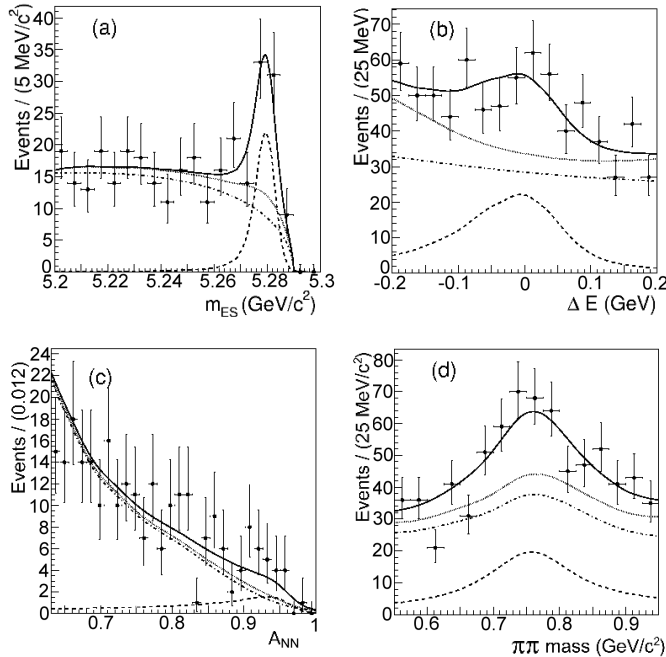


FIG. 1: Likelihood projection plots for the four fit variables, (a) m_{ES} , (b) ΔE , (c) A_{NN} , and (d) $m_{\pi\pi}$. Each plot shows the total PDF (solid line), total background (dotted line), continuum contribution (dotted-dashed line), and the signal component (dashed line).

Corrections to the π^0 energy resolution and efficiency, determined using various data control samples, add a systematic uncertainty of 7.2%. A relative systematic uncertainty of 1% is assumed for the pion identification. A relative systematic uncertainty of 0.8% on the efficiency for a single charged track is applied. Adding all the above contributions in quadrature gives a relative systematic uncertainty on the branching fraction of 7.3%. Another contribution of 1.1% comes from the uncertainty on the total number of B events.

To calculate the effects of systematic shifts in the charge asymmetries of background modes, the asymmetry of each mode is varied by its measured uncertainty. For contributions with no asymmetry measurement, we assume zero asymmetry and assign an uncertainty of 20%, motivated by the largest charge asymmetry measured in any mode so far [15]. The individual shifts are then added in quadrature to find the total systematic uncertainty. In addition, the effect of altering the normalizations of the B backgrounds affects the fitted asymmetry. The size of the shift on the fitted \mathcal{A}_{CP} is taken as the size of the systematic uncertainty.

The central value of the signal yield from the maximum likelihood fit is 365 ± 49 events, with a background of 44840 ± 217 continuum events and an expected background of 842 ± 34 events from other B decays. Fig. 1 shows the distributions of m_{ES} , ΔE , A_{NN} and $m_{\pi\pi}$. The plots are enhanced in signal by selecting only those events which exceed a threshold of 0.1 (0.05 for A_{NN}) for the likelihood ratio [16] $R = (N^{\text{Sig}} \mathcal{P}^{\text{Sig}}) / (N^{\text{Sig}} \mathcal{P}^{\text{Sig}} + \sum_i N_i^{\text{Bkg}} \mathcal{P}_i^{\text{Bkg}})$, where N are the central values of the yields from the fit and \mathcal{P} are the PDFs with the projected variable integrated out. This threshold is optimized by maximizing the ratio $S = (N^{\text{Sig}} \epsilon^{\text{Sig}}) / \sqrt{N^{\text{Sig}} \epsilon^{\text{Sig}} + \sum_i N_i^{\text{Bkg}} \epsilon_i^{\text{Bkg}}}$ where ϵ are the efficiencies after the threshold is applied. The PDF components are then scaled by the appropriate ϵ . The efficiencies for the likelihood ratios vary for each variable and result in a different number of events in each projection. Compared against the null hypothesis, the statistical significance $\sqrt{-2 \ln(\mathcal{L}_{\text{Null}} / \mathcal{L}_{\text{Max}})}$ of the signal yield amounts to 8.7 standard deviations. We obtain $\mathcal{B}(B^\pm \rightarrow \rho^\pm \pi^0) = [10.2 \pm 1.4 \pm 0.9] \times 10^{-6}$, and $\mathcal{A}_{CP} = -0.01 \pm 0.13 \pm 0.02$, where the first error is statistical and the second error systematic. The measurements are consistent with previous results [5] and provide improved constraints for the determination of the angle α from $B \rightarrow \rho\pi$ decays.

We are grateful for the excellent luminosity and machine conditions provided by our PEP-II colleagues, and for the substantial dedicated effort from the computing organizations that support BABAR. The collaborating institutions wish to thank SLAC for its support and kind hospitality. This work is supported by DOE and NSF (USA), NSERC (Canada), IHEP (China), CEA and CNRS-IN2P3 (France), BMBF and DFG (Germany), INFN (Italy), FOM (The Netherlands), NFR (Norway), MIST (Russia), and PPARC (United Kingdom). Individuals have received support from CONACyT (Mexico), A. P. Sloan Foundation, Research Corporation, and Alexander von Humboldt Foundation.

[1] N. Cabibbo, Phys. Rev. Lett. **10**, 531 (1963).

[2] M. Kobayashi and T. Maskawa, Prog. Theor. Phys. **49**,

652 (1973).

[3] BABAR Collaboration, B. Aubert *et al.*, Phys. Rev. Lett.

- 89**, 201802 (2002).
- [4] A. Snyder and H. Quinn, Phys. Rev. D **48**, 2139 (1993).
- [5] BABAR Collaboration, B. Aubert *et al.*, Phys. Rev. Lett. **93**, 051802 (2004).
- [6] Belle Collaboration, J. Zhang *et al.*, Phys. Rev. Lett. **94**, 031801 (2005).
- [7] BABAR Collaboration, B. Aubert *et al.*, Nucl. Instrum. Methods **A479**, 1 (2002).
- [8] G. Hanson *et al.*, Phys. Rev. Lett. **35**, 1609 (1975).
- [9] BABAR Collaboration, B. Aubert *et al.*, Phys. Rev. Lett. **91**, 201802 (2003).
- [10] Particle Data Group, S. Eidelman *et al.*, Phys. Lett. B **592**, 1 (2004).
- [11] BABAR Collaboration, B. Aubert *et al.*, Phys. Rev. Lett. **97**, 051802 (2006).
- [12] K. Cranmer, Comput. Phys. Commun. **136**, 198 (2001).
- [13] ARGUS Collaboration, H. Albrecht *et al.*, Phys. Lett. B **241**, 278 (1990).
- [14] T. Skwarnicki, Ph.D. thesis, Cracow Institute of Nuclear Physics, DESY-F31-86-02, 1986.
- [15] BABAR Collaboration, B. Aubert *et al.*, Phys. Rev. Lett. **93**, 131801 (2004).
- [16] BABAR Collaboration, B. Aubert *et al.*, Phys. Rev. D **71**, 111101 (2005).